www.nature.com/aps

Acta Pharmacologica Sinica

ARTICLE

Inhibition of miR-135a-5p attenuates vascular smooth muscle cell proliferation and vascular remodeling in hypertensive rats

Chao Ye[1], Ying Tong[1], Nan Wu[1], Guo-wei Wan[1], Fen Zheng[1], Jing-yu Chen[1], Jian-zhen Lei[1], Hong Zhou[1], Ai-dong Chen[1], Jue-jin Wang[1], Qi Chen[2], Yue-hua Li[2], Yu-ming Kang[3] and Guo-qing Zhu[1,2]

Proliferation of vascular smooth muscle cells (VSMCs) greatly contributes to vascular remodeling in hypertension. This study is to determine the roles and mechanisms of miR-135a-5p intervention in attenuating VSMC proliferation and vascular remodeling in spontaneously hypertensive rats (SHRs). MiR-135a-5p level was raised, while fibronectin type III domain-containing 5 (FNDC5) mRNA and protein expressions were reduced in VSMCs of SHRs compared with those of Wistar–Kyoto rats (WKYs). Enhanced VSMC proliferation in SHRs was inhibited by miR-135a-5p knockdown or miR-135a-5p inhibitor, but exacerbated by miR-135a-5p mimic. VSMCs of SHRs showed reduced myofilaments, increased or even damaged mitochondria, increased and dilated endoplasmic reticulum, which were attenuated by miR-135a-5p inhibitor. Dual-luciferase reporter assay shows that FNDC5 was a target gene of miR-135a-5p. Knockdown or inhibition of miR-135a-5p prevented the FNDC5 downregulation in VSMCs of SHRs, while miR-135a-5p mimic inhibited FNDC5 expressions in VSMCs of both WKYs and SHRs. FNDC5 knockdown had no significant effects on VSMC proliferation of WKYs, but aggravated VSMC proliferation of SHRs. Exogenous FNDC5 or FNDC5 overexpression attenuated VSMC proliferation of SHRs, and prevented miR-135a-5p mimic-induced enhancement of VSMC proliferation of SHR. MiR-135a-5p knockdown in SHRs attenuated hypertension, normalized FNDC5 expressions and inhibited vascular smooth muscle proliferation, and alleviated vascular remodeling. These results indicate that miR-135a-5p promotes while FNDC5 inhibits VSMC proliferation in SHRs. Silencing of miR-135a-5p attenuates VSMC proliferation and vascular remodeling in SHRs via disinhibition of FNDC5 transcription. Either inhibition of miR-135a-5p or upregulation of FNDC5 may be a therapeutically strategy in attenuating vascular remodeling and hypertension.

Keywords: microRNA; FNDC5; hypertension; vascular smooth muscle cells; proliferation; vascular remodeling

Acta Pharmacologica Sinica (2021) 42:1798–1807; https://doi.org/10.1038/s41401-020-00608-x

INTRODUCTION

Vascular smooth muscle cells (VSMCs) are the main cell components of the media of arteries. VSMC proliferation plays pivotal roles in arterial stiffness and vascular remodeling in a variety of vascular diseases, including hypertension, atherosclerosis, restenosis after angioplasty or bypass, transplantation arteriopathy, and diabetic vascular complications [1, 2]. Vascular remodeling is thought to play protective roles in the short term but pathological roles in the long term, and these pathological roles of vascular remodeling are associated with increased risks of cardiovascular events [3]. Reversing the vascular remodeling associated with hypertension is important for preventing the progression of hypertension [4].

MicroRNAs (miRNAs) are endogenous noncoding, single-stranded, small RNAs that post-transcriptionally inhibit the expression of target genes by binding to the 3′-untranslated regions (3′-UTRs) of target mRNA sequence [5]. Some miRNAs are important therapeutic targets or biomarkers of several diseases [6–8]. Recent studies in our lab have shown that miR-155-5p in the extracellular vesicles-derived from adventitial fibroblasts (AFs) attenuates VSMC proliferation by inhibiting angiotensin-converting enzyme (ACE) expression in spontaneously hypertensive rats (SHRs) [9, 10]. It has been shown that miR-135a-5p promotes the proliferation of lung cancer cells [11] and human adipose-derived mesenchymal stem cells [12] but inhibits the proliferation of neck squamous cell carcinoma cells [13] and thyroid carcinoma cells [14]. However, the role of miR-135a-5p in VSMC proliferation is still unknown.

Fibronectin type III domain-containing 5 (FNDC5), a precursor of irisin, is a transmembrane protein encoded by the FNDC5 gene [15]. Our previous studies have shown that FNDC5/irisin attenuates insulin resistance and hepatosteatosis and improves glucose and lipid metabolism [16–18]. Moreover, FNDC5 inhibits adipose tissue inflammation in obese rats [19] and in the AFs of SHRs [20]. Irisin reduces infarct size and improves cardiac function in the hearts of mice with myocardial infarction [21]. Analysis with TargetScanHuman, an online tool that predicts miRNA targets in mammals, suggests that FNDC5 might be one of the targets of

[1]Department of Physiology, Key Laboratory of Targeted Intervention of Cardiovascular Disease, Collaborative Innovation Center of Translational Medicine for Cardiovascular Disease, Nanjing Medical University, Nanjing 211166, China; [2]Department of Pathophysiology, Nanjing Medical University, Nanjing 211166, China and [3]Department of Physiology and Pathophysiology, Cardiovascular Research Center, Xi'an Jiaotong University School of Medicine, Xi'an 710061, China
Correspondence: Guo-qing Zhu (gqzhucn@njmu.edu.cn)
These authors contributed equally: Chao Ye, Ying Tong.

Received: 8 September 2020 Accepted: 29 December 2020
Published online: 15 February 2021

miR-135a-5p. The present study was designed to investigate the roles of miR-135a-5p and its interaction with FNDC5 in VSMC proliferation and vascular remodeling in SHRs. The therapeutic effects of miR-135a-5p knockdown on VSMC proliferation, vascular remodeling, and hypertension were investigated in SHRs.

MATERIALS AND METHODS

Experimental animals

Nine-week-old male Wistar–Kyoto rats (WKYs) and SHRs (Vital River Laboratory Animal Technology Co., Ltd., Beijing, China) were used in the present study. The rats were housed in a temperature-controlled room with a 12-h light/12-h dark cycle. The rats were provided normal rat chow and tap water ad libitum. The experiments were conducted according to the principles of the Guide for the Care and Use of Laboratory Animals (NIH, 8th edition, 2011) and approved by the Experimental Animal Care and Use Committee of Nanjing Medical University. The systolic blood pressures of the SHRs used in the present study were higher than 150 mmHg. The rats were euthanized with an overdose of pentobarbital sodium (200 mg/kg, iv; Sigma Chemical Co., St. Louis, MO, USA) at the end of the experiment.

Culture of VSMCs

VSMCs were harvested from the aortas of WKYs and SHRs as we previously described [22]. In brief, rat thoracic aortas were isolated, and perivascular fat tissues were removed. Each aorta was longitudinally cut open and stripped of its intima. The aortic media was carefully separated and treated with 0.4% collagenase in DMEM for 30 min. After centrifugation, the cells were resuspended in DMEM supplemented with 10% fetal bovine serum (FBS), penicillin (100 IU/mL), and streptomycin (10 mg/mL) and incubated at 37 °C in an incubator with 5% CO_2. VSMCs were identified by positive α-SMA (a marker of VSMCs) staining and negative vimentin (a marker of fibroblasts) and PECAM-1 (a marker of endothelial cells) staining. Primary VSMCs from the third to the fifth passages were used in this study. The same number of VSMCs from the same passage after isolation from WKYs and SHRs were seeded into 96-well plates. After reaching approximately 70% confluence, the VSMCs were starved in DMEM containing 0.1% FBS for 24 h.

Evaluation of VSMC proliferation

First, VSMC proliferation was measured with a cell counting kit-8 (CCK-8) kit (Beyotime Biotechnology, Shanghai, China) following the manufacturer's instructions. A microplate reader (Model ELX800, BioTek, Vermont, USA) was used to measure the absorbance at 450 nm [23]. Second, VSMC proliferation was evaluated with a 5-ethynyl-2′-deoxyuridine (EdU) incorporation assay, which examines DNA synthesis using the Cell-Light™ EdU Apollo®567 In Vitro Imaging Kit (Guangzhou RiboBio, Guangzhou, China). The number of EdU-positive cells was normalized to the total number of cells [24]. Finally, proliferating cell nuclear antigen (PCNA) protein expression was examined by Western blotting [23].

Transmission electron microscopy

Transmission electronic microscopy was used to observe the ultrastructural alterations in the VSMCs from WKYs and SHRs. The VSMCs were collected after centrifugation at 4 °C, and then, the VSMCs were fixed in a fixative (G1124; Wuhan Servicebio Co., Ltd; Wuhan, China), embedded in 2% low melting point agarose, dehydrated with an graded series of ethanol, permeabilized with resin and embedded into a special capsule. The resin blocks were cut into 80-nm thin sections by a Leica Ultra Microtome (Leica UC7; Wetzlar, Germany) after polymerization treatment. Images were acquired by transmission electron microscopy (HT7800; Hitachi, Tokyo, Japan).

Transfection of miR-135a-5p mimic and inhibitor

The RNAifectin™ transfection reagent, negative control (NC), miR-135a-5p mimic, and miR-135a-5p inhibitor were obtained from Applied Biological Materials Inc. (Richmond, BC, Canada). VSMCs were seeded into a 6-well plate (approximately 5×10^5 cells/well) and cultured for 16 h. The cells were transfected with the RNAifectin™ transfection reagent (6 μL) plus the miR-135a-5p mimic (50 nmol/L), the miR-135a-5p inhibitor (100 nmol/L), or their corresponding NC for 6 h. Then, the culture medium was replaced to remove the transfection reagent. The measurements were conducted 24 h after the transfection.

Knockdown of miR-135a-5p in VSMCs and rats

Commercial lentiviral vectors targeting miR-135a-5p (miR-135a-5p siRNA) and scrambled siRNA (Scr-siRNA, an NC) were obtained from Genomeditech Co., Ltd. (Shanghai, China). For VSMCs, the cells were transfected with Scr-siRNA or miR-135a-5p siRNA (40 MOI) in 6-well plates. For WKYs and SHRs, each rat received an intravenous injection of miR-135a-5p siRNA or Scr-siRNA (2×10^{11} plaque forming units/mL, 100 μL). The sequence of miR-135a-5p siRNA was 5′-TATGGCTTTTTATTCCTATGTGA-3′.

FNDC5 knockdown in VSMCs

Lentiviral vectors targeting FNDC5 (FNDC5-siRNA, 1×10^9 TU/mL) and Scr-siRNA were constructed and identified by GeneChem Co., Ltd. (Shanghai, China). The nucleotide sequence of FNDC5-siRNA was 5′-GGCCGAGAAGATGGCCTCTAA-3′. VSMCs were infected with Scr-siRNA or FNDC5-siRNA (MOI = 80) with polybrene.

FNDC5 overexpression in VSMCs

The FNDC5 overexpression plasmid (FNDC5-OE, 1 mg/L) was constructed and identified by GeneChem Co., Ltd. An empty plasmid was used as the NC (Ctrl). Lipofectamine 3000 (Invitrogen, Carlsbad, CA, USA) and 1 mg/L plasmid were used for the transfection, according to the manufacturer's protocols.

Quantification of miR-135a-5p by qPCR

The miR-135a-5p levels in the VSMCs, aortas, and mesenteric arteries (MAs) were reexamined with qPCR. Total RNA was extracted with a miRcute miRNA isolation kit and quantified with a NanoDrop 2000 Spectrophotometer (Thermo Fisher Scientific, Wilmington, DE, USA). The starting concentrations of the total RNA were the same for all the samples. The RNA was reverse-transcribed to cDNA with a miRcute Plus miRNA First-Strand cDNA Kit. The miRNAs were quantitatively detected with a MiRcute Plus miRNA qPCR Kit containing the QuantiTect SYBR Green PCR Master Mix, the miScript Universal Primer, and the miRNA-specific primer. The StepOnePlus™ Real-Time PCR System (Applied Biosystems, Foster City, CA, USA) was used for the amplification and detection of the PCR products. The U6 small RNA expression level was utilized to normalize the miR-135a-5p expression levels. All the commercial kits used for qPCR were obtained from Tiangen Biotech Co., Ltd. (Beijing, China). The primers for miR-135a-5p and U6 were 5′-GTGGTTTGTCCAAACTCATC-3′ and 5′-TTGGAACGATACAGAGAAGATTAGCAT-3′, respectively.

Measurement of the FNDC5 mRNA levels by qPCR

The FNDC5 mRNA levels in the VSMCs, aortas, and MAs were measured with qPCR. Total RNA was extracted with TRIzol reagent (Life Technologies, Gaithersburg, MD, USA). Reverse transcriptase reactions were performed with PrimeScript® RT reagent kits (Takara Bio Inc, Otsu, Shiga, Japan) and a StepOnePlus™ Real-Time PCR System. Quantitative measurements were performed with SYBR Green qPCR (Takara Biotechnology Co., Ltd., Tokyo, Japan) using the StepOnePlus system, and target gene expression was normalized to GAPDH expression. The primer sequences for qPCR are listed in Supplementary Table S1.

Western blot analysis

The protein expression of FNDC5 and PCNA in the VSMCs was examined by Western blot analysis. The total protein concentrations in the supernatants of the samples were determined with a BCA protein assay kit (Thermo Fisher Scientific, Rockford, IL, USA). The proteins were separated by SDS-PAGE and then transferred to PVDF membranes. The antibodies against FNDC5 and β-actin were purchased from Abcam (ab174833; Abcam, Cambridge, MA, USA) and Cell Signaling Technology (8457; CST, Beverly, MA, USA), respectively. The antibodies against PCNA were obtained from Protein Tech Group Inc. (Chicago, IL, USA). The secondary antibodies were acquired from Santa Cruz Biotechnology Inc. (Santa Cruz, CA, USA).

Immunohistochemistry

Immunohistochemistry was utilized to detect the expression of FNDC5 and PCNA in the aortas and MAs of WKYs and SHRs, as we previously reported [9]. The primary anti-FNDC5 antibody (1:100) was obtained from Abcam. The primary anti-PCNA antibody (1:100) was acquired from Protein Tech Group Inc. The horseradish peroxidase-conjugated goat anti-rabbit antibody was obtained from Santa Cruz Biotechnology Inc. 3,3-Diaminobenzidine was used to show the positive cells. The sections were counterstained with hematoxylin, and the images were captured with a light microscope (BX-51, Olympus, Tokyo, Japan). The quantitative analysis was performed with ImageJ software (v1.80; NIH, Bethesda, Maryland).

Dual-luciferase reporter assay

The 3′-UTR dual-luciferase reporter vectors containing the 3′-UTR of FNDC5 with wild-type (WT) and mutant (Mut) miR-135a-5p binding sites were separately constructed (Genomeditech, Shanghai, China). All the constructs containing 3′-UTR inserts were sequenced and validated. VSMCs were seeded in 24-well plates 24 h prior to transfection. Subsequently, the cells were cotransfected with either the WT or Mut luciferase reporter plasmids plus miR-NC or pre-miR-135a-5p using Lipofectamine 3000, according to the manufacturer's instructions. The luciferase activities were measured 24 h after transfection using the Dual-Luciferase Reporter Assay System (Promega, Madison, WI, USA) on a Luminometer 20/20n (Turmer Biosystems, Sunnyvale, CA, USA). The Renilla luciferase activity was used as the internal control to determine transfection efficiency and cell density.

Masson's staining

Sections of aortas and MAs from WKYs and SHRs were subjected to Masson's trichrome staining, as we previously reported [25]. Images were captured with a light microscope, and quantitative analysis was performed with ImageJ software. Vascular remodeling was evaluated based on the media thickness, the lumen diameter, the ratio of media thicknesses to lumen diameter, the outer diameter, and the media cross-sectional area.

Blood pressure measurement

The blood pressure of the tail artery was examined every week in conscious WKYs and SHRs with a noninvasive computerized tail-cuff system (NIBP, ADInstruments, Sydney, New South Wales, Australia), as we previously reported [26]. The blood pressure and heart rate values were calculated by averaging six measurements.

Statistical analysis

The experiments were performed in a randomized, double-blinded fashion. The data are expressed as the mean ± SEM. Student's unpaired *t*-test was used to compare differences between two groups. One-way or two-way ANOVA followed by post hoc Bonferroni test was used for multiple comparisons. $P < 0.05$ was considered statistically significant.

RESULTS

Effects of miR-135a-5p on VSMC proliferation

VSMC proliferation was evaluated with a CCK-8 kit, EdU staining, and PCNA expression analysis. Knockdown of miR-135a-5p attenuated the VSMC proliferation in SHRs (Fig. 1a). The efficacy was confirmed by the finding that miR-135a-5p siRNA significantly reduced the miR-135a-5p levels in the VSMCs of both the WKYs and SHRs (Supplementary Fig. S1). The miR-135a-5p inhibitor showed inhibitory effects similar to those of miR-135a-5p siRNA (Supplementary Fig. S2), and the miR-135a-5p mimic promoted the VSMC proliferation in the SHRs (Fig. 1b). However, these treatments had no significant effects on the VSMC proliferation in the WKYs. These results indicate that miR-135a-5p promotes VSMC proliferation in SHRs and that endogenous miR-135a-5p at least partially contributes to the enhanced VSMC proliferation in SHRs.

Effects of the miR-135a-5p inhibitor on VSMC ultrastructure

Ultrastructure was observed by transmission electron microscopy. VSMC proliferation is characterized by reduced myofilaments and increased and dilated endoplasmic reticulum cytoplasm [27, 28]. Cell hypertrophy is characterized by enlarged cells and nuclei and increased numbers of individual mitochondria [29, 30]. In VSMCs of WKYs, the number and distribution of organelles were normal, and the cytoplasm was filled with myofilaments (Fig. 2a, e). Treatment with the miR-135a-5p inhibitor had no obvious effects on the ultrastructure of the WKY VSMCs (Fig. 2b, f). In contrast to the VSMCs from the WKYs, the VSMCs from the SHRs exhibited reduced cytoplasmic myofilaments, increased numbers of mitochondria, including damaged mitochondria, and increased and dilated endoplasmic reticulum (Fig. 2c, g); these effects were attenuated by treatment with the miR-135a-5p inhibitor (Fig. 2d, h). The ultrastructural alterations indicate that VSMC proliferation is enhanced in SHRs and that inhibition of miR-135a-5p attenuates VSMC proliferation in SHRs.

MiR-135a-5p levels and FNDC5 expression in VSMCs

MiR-135a-5p levels in the VSMCs from the SHRs were higher than those in the VSMCs from the WKYs (Fig. 3a). To identify the target via which miR-135a-5p promotes VSMC proliferation, we searched for the possible targets of miR-135a-5p in TargetScanHuman, an online tool that predicts miRNA targets (http://www.targetscan.org/). Among the variety of possible targets, FNDC5 was one of the possible targets of miR-135a-5p in which we became greatly interested because we have previously shown its beneficial roles in attenuating disordered glucose/lipid metabolism, insulin resistance, and inflammation in obesity and diabetes [16–19]. According to TargetScanHuman, the predicted site of this interaction is position 2030–2036 of the FNDC5 3′-UTR (Fig. 3b). To test this possibility, a dual-luciferase reporter assay was performed in VSMCs of WKYs. Luciferase reporter assays are widely used to identify the target genes of miRNAs [31, 32]. We found that the firefly luciferase activity was inhibited when the cells were cotransfected with pre-miR-135a-5p (Fig. 3c). Furthermore, the FNDC5 mRNA and protein expression was reduced in the VSMCs from the SHRs compared with that in the VSMCs from the WKYs (Fig. 3d). These findings suggest that FNDC5 is a target gene of miR-135a-5p.

Effects of miR-135a-5p on FNDC5 expression

Either miR-135a-5p knockdown or the miR-135a-5p inhibitor reversed the downregulation of FNDC5 mRNA and protein expression in the VSMCs from the SHRs but had no significant effects on FNDC5 expression in the VSMCs from the WKYs (Fig. 4a, b). The efficacy of miR-135a-5p knockdown was confirmed by the finding that miR-135a-5p siRNA significantly reduced the miR-135a-5p levels in the VSMCs from both the WKYs and SHRs (Supplementary Fig. S3). The miR-135a-5p mimic inhibited FNDC5

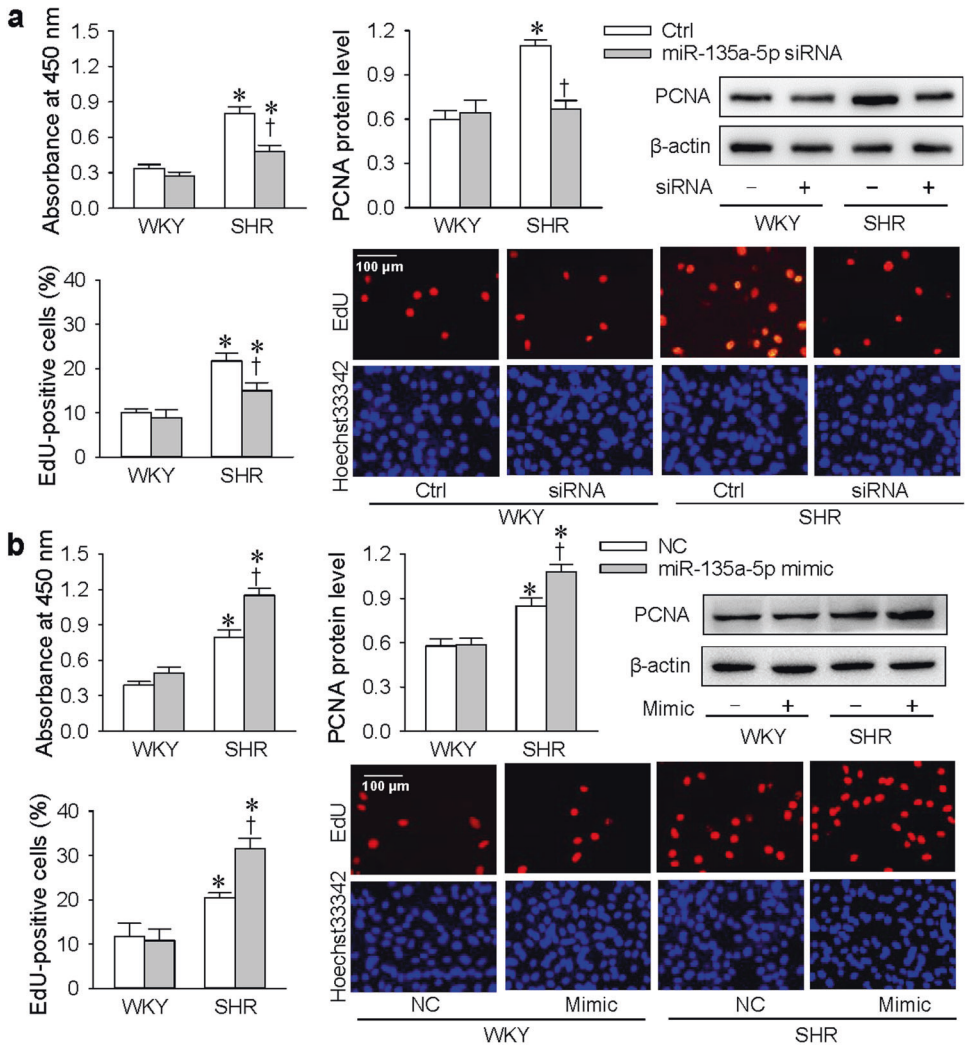

Fig. 1 Effects of miR-135a-5p on VSMC proliferation in WKYs and SHRs. VSMC proliferation was evaluated with CCK-8 kits, EdU incorporation assays, and PCNA protein expression analysis. **a** Effects of miR-135a-5p siRNA on VSMC proliferation. Measurements were carried out 48 h after treatment with control lentivirus (Ctrl) or miR-135a-5p siRNA (40 MOI). **b** Effects of the miR-135a-5p mimic on VSMC proliferation. Measurements were made 24 h after treatment with NC (50 nmol/L) or miR-135a-5p mimic (50 nmol/L). The values are mean ± SEM. $^{*}P < 0.05$ vs WKY. $^{\dagger}P < 0.05$ vs Ctrl or NC. $n = 4–6$

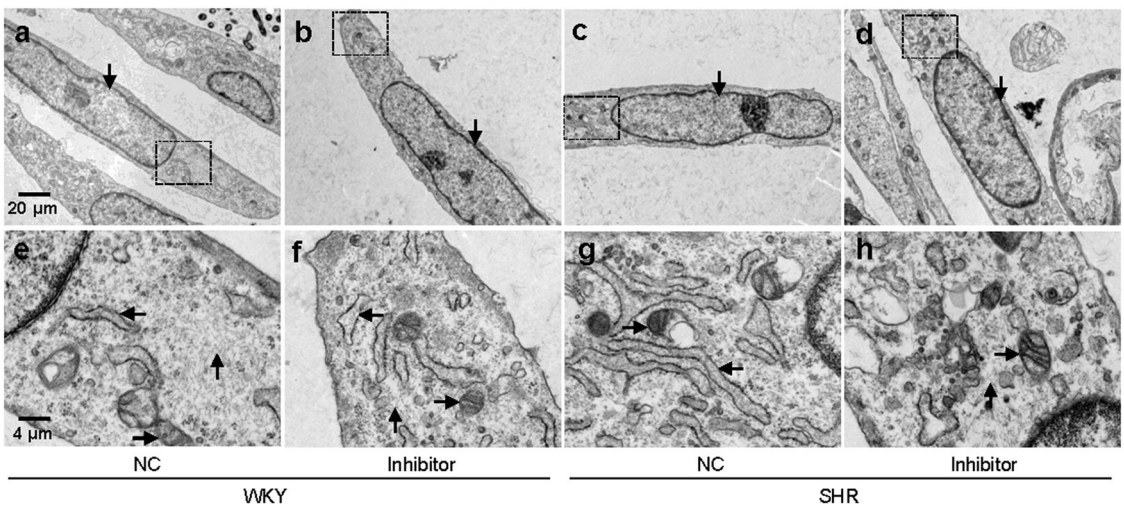

Fig. 2 Ultrastructural alterations induced by the miR-135a-5p inhibitor in the VSMCs of WKYs and SHRs. The ultrastructure was detected by transmission electron microscopy (TEM). The VSMCs were treated with negative control (NC, 100 nmol/L) or miR-135a-5p inhibitor (100 nmol/L) for 24 h. **a**–**d** TEM images at 1000× magnification. The down arrow indicates the nucleus. **e**–**h** TEM images at 5000× magnification of the boxed area in the upper images. The up arrow indicates cytoplasmic filament; the arrow to the right indicates mitochondria; and the arrow to the left indicates the endoplasmic reticulum

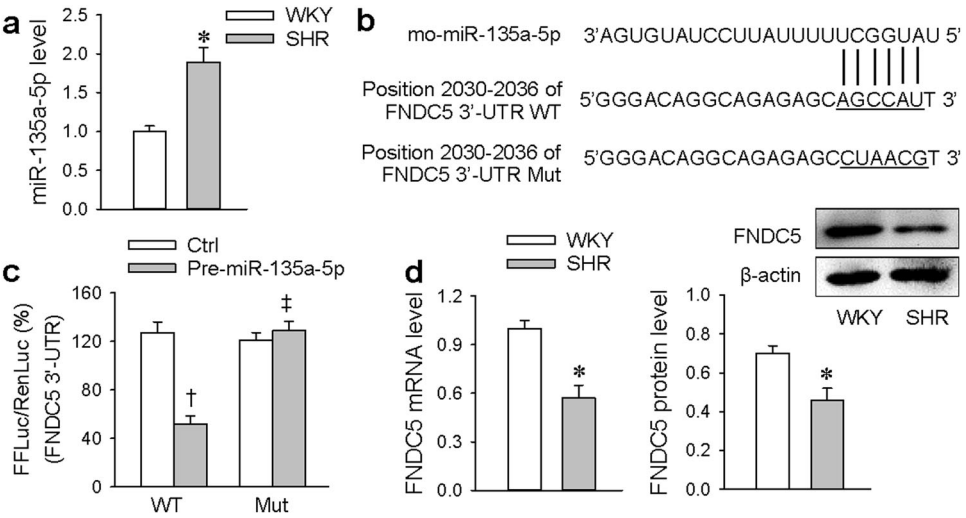

Fig. 3 MiR-135a-5p and FNDC5 expression in the VSMCs of WKYs and SHRs. a Relative miR-135a-5p expression values measured by qPCR. **b** Prediction of the miR-135a-5p binding site by TargetScanHuman. **c** Dual-luciferase reporter assay shows that FNDC5 is a target of miR-135a-5p in VSMCs of WKYs. FFLuc, firefly luciferase; RenLuc, renilla luciferase; WT, wild-type; Mut, mutant. **d** Relative FNDC5 mRNA and protein expression values. The values are the mean ± SEM. *$P < 0.05$ vs WKY. †$P < 0.05$ vs Ctrl. ‡$P < 0.05$ vs WT. $n = 6$

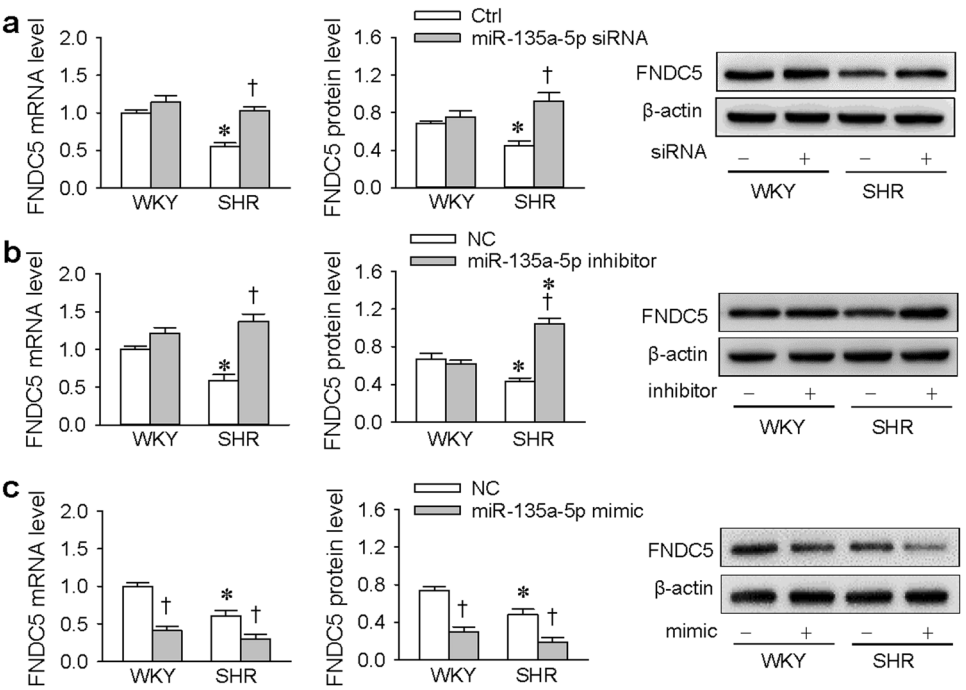

Fig. 4 Effects of miR-135a-5p on FNDC5 expression in the VSMCs of WKYs and SHRs. a Effects of miR-135a-5p siRNA on the FNDC5 mRNA and protein expression in VSMCs. The measurements were carried out 48 h after treatment with control lentivirus (Ctrl) or miR-135a-5p siRNA (40 MOI). **b** Effects of the miR-135a-5p inhibitor on the FNDC5 mRNA and protein expression in VSMCs. Measurements were performed 24 h after treatment with the negative control (NC, 100 nmol/L) or miR-135a-5p inhibitor (100 nmol/L). **c** Effects of the miR-135a-5p mimic on the FNDC5 mRNA and protein expression in VSMCs. The measurements were carried out 24 h after treatment with the NC (50 nmol/L) or miR-135a-5p mimic (50 nmol/L). The values are the mean ± SEM. *$P < 0.05$ vs WKY. †$P < 0.05$ vs Ctrl or NC. $n = 4$

mRNA and protein expression in the VSMCs from both the WKYs and SHRs (Fig. 4c). These results provide solid evidence that miR-135a-5p inhibits FNDC5 expression and that the increased miR-135a-5p levels in SHRs are responsible for FNDC5 downregulation in the VSMCs from SHRs.

Effects of FNDC5 knockdown on VSMC proliferation

FNDC5-siRNA reduced the FNDC5 protein expression in the VSMCs from both the WKYs and SHRs (Supplementary Fig. S4a). FNDC5 knockdown had no significant effects on the proliferation of VSMCs from WKYs but increased the proliferation of VSMCs from SHRs (Fig. 5a–c and Supplementary Fig. S4b). The findings suggest that endogenous FNDC5 still plays a role in inhibiting VSMC proliferation in SHRs, although FNDC5 expression is reduced in the VSMCs of SHRs.

Effects of exogenous FNDC5 on VSMC proliferation

The application of FNDC5 had no significant effect on the proliferation of VSMCs from WKYs but attenuated the proliferation of VSMCs from SHRs (Fig. 6a and Supplementary Fig. S5a). The

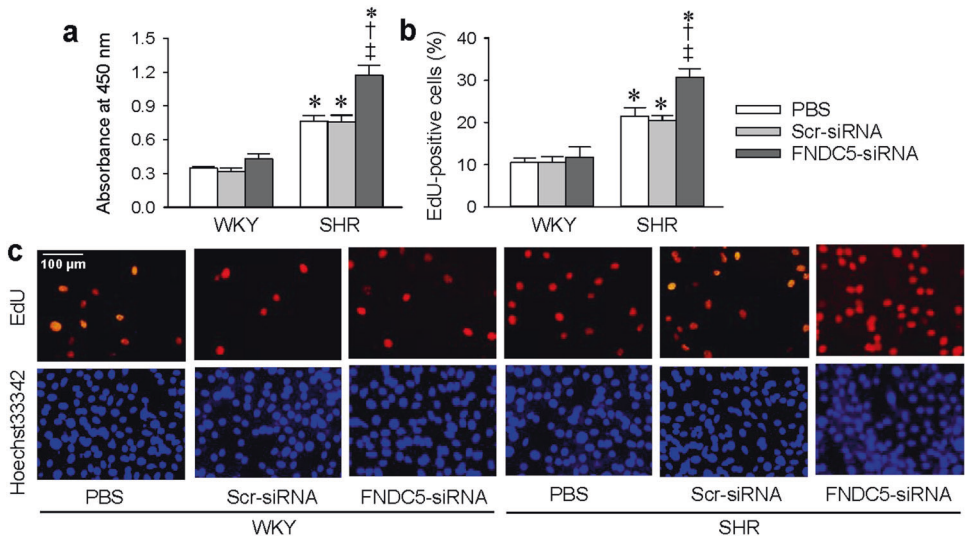

Fig. 5 Effects of FNDC5 knockdown on the VSMC proliferation in WKYs and SHRs. Proliferation was evaluated with CCK-8 kits (**a**) and EdU incorporation assays (**b**, **c**).The measurements were carried out 48 h after treatment with PBS, control lentivirus (Scr-siRNA, 80 MOI) or FNDC5-siRNA (80 MOI). The values are the mean ± SEM. $^{*}P < 0.05$ vs WKY. $^{\dagger}P < 0.05$ vs PBS. $^{\ddagger}P < 0.05$ vs Scr-siRNA. $n = 4–6$

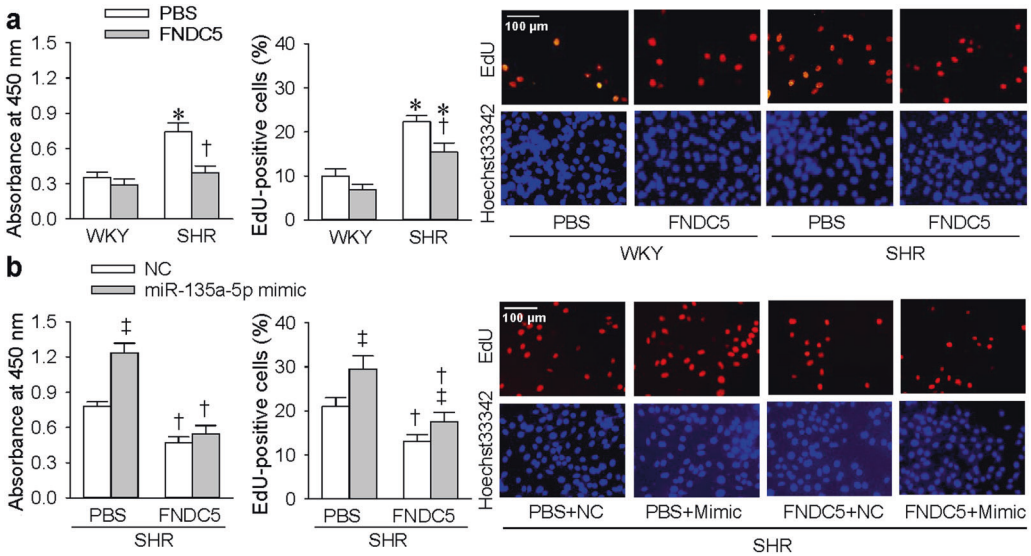

Fig. 6 Effects of FNDC5 on VSMC proliferation. Proliferation was evaluated with CCK-8 kits and EdU incorporation assays. **a** Effects of FNDC5 on the VSMC proliferation in WKYs and SHRs. The measurements were carried out 24 h after treatment with PBS or FNDC5 (200 nmol/L). **b** Effects of FNDC5 on the miR-135a-5p-induced VSMC proliferation in SHRs. The measurements were carried out 24 h after treatment with PBS or FNDC5 (200 nmol/L) plus negative control (NC, 50 nmol/L) or miR-135a-5p mimic (50 nmol/L). The values are the mean ± SEM. $^{*}P < 0.05$ vs WKY. $^{\dagger}P < 0.05$ vs PBS. $^{\ddagger}P < 0.05$ vs NC. $n = 4–6$

results suggest that FNDC5 upregulation may be a therapeutic strategy for attenuating VSMC proliferation during hypertension. Moreover, exogenous FNDC5 prevented the miR-135a-5p mimic-induced VSMC proliferation in the SHRs (Fig. 6b and Supplementary Fig. S5b). The findings indicate that the role of miR-135a-5p in promoting VSMC proliferation in SHRs is mediated by the negative regulation of FNDC5 expression in SHRs.

Effects of FNDC5 overexpression on VSMC proliferation

Transfection with the FNDC5 overexpression plasmid increased the FNDC5 protein expression in both the control- and miR-135a-5p mimic-treated VSMCs from the SHRs, confirming the efficacy of FNDC5 overexpression (Fig. 7a). FNDC5 overexpression attenuated VSMC proliferation in the SHRs (Fig. 7b–e).

Effects of miR-135a-5p knockdown on blood pressure and FNDC5 expression

The intravenous injection of lentiviral vectors carrying Scr-siRNA or siRNA-targeting miR-135a-5p (miR-135a-5p siRNA) was carried out in WKYs and SHRs. The blood pressure of the rats was measured every week. MiR-135a-5p knockdown attenuated hypertension in the SHRs 2 weeks after the injection but had almost no effects on blood pressure during the first week (Fig. 8a). All the other measurements were conducted at the end of the third week. The miR-135a-5p levels in both the aortas and MAs of the WKYs and SHRs were reduced, confirming the efficacy of miR-135a-5p knockdown (Fig. 8b). MiR-135a-5p knockdown normalized the FNDC5 mRNA and protein expression in the aortas and MAs of the SHRs, but no significant effects were observed in the aortas and

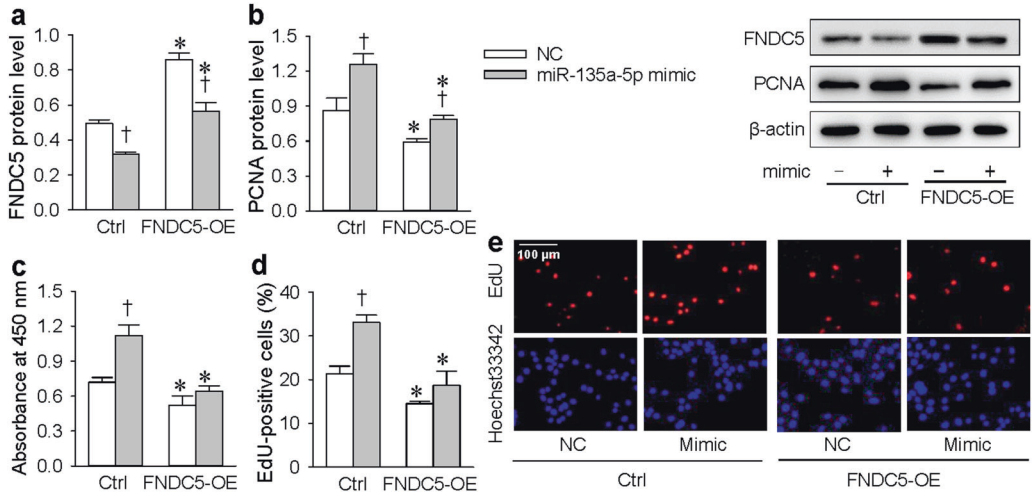

Fig. 7 Effects of FNDC5 overexpression on the VSMC proliferation in SHRs. The measurements were carried out 24 h after treatment with the control plasmid (Ctrl, 1 mg/L) or FNDC5 overexpression plasmid (FNDC5-OE, 1 mg/L) plus negative control (NC, 50 nmol/L) or miR-135a-5p mimic (50 nmol/L). **a** FNDC5 protein expression. **b**–**e** VSMC proliferation was evaluated by PCNA protein expression analysis (**b**), CCK-8 kits (**c**) and EdU incorporation assays (**d, e**). The values are the mean ± SEM. $^{*}P < 0.05$ vs Ctrl. $^{\dagger}P < 0.05$ vs NC. $n = 4$–6

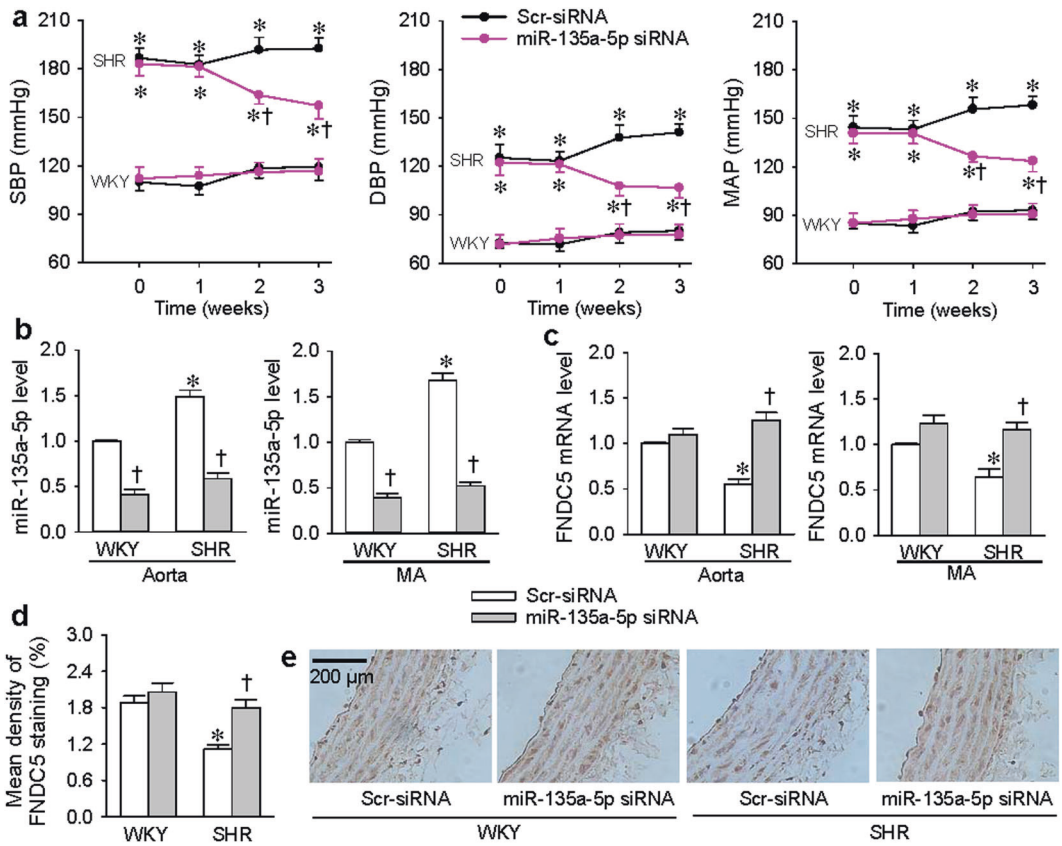

Fig. 8 Effects of miR-135a-5p knockdown in WKYs and SHRs on blood pressure and miR-135a-5p and FNDC5 expression. The rats were subjected to intravenous injection of control lentivirus (Scr-siRNA) or miR-135a-5p siRNA lentivirus (miR-135a-5p siRNA, 2×10^{11} plaque forming units/mL, 100 μL). **a** The systolic blood pressure (SBP), diastolic blood pressure (DBP), and mean arterial pressure (MAP) were measured once a week in conscious rats. **b** MiR-135a-5p levels in the aortas and mesenteric arteries (MAs). **c** FNDC5 mRNA levels in the aortas and MAs. **d** Bar graph showing the relative densities of FNDC5 staining in the aortas. **e** Representative images of immunohistochemical analysis of FNDC5 (brown color) in the aortas. The values are the mean ± SE. $^{*}P < 0.05$ vs WKY. $^{\dagger}P < 0.05$ vs Scr-siRNA. $n = 6$

MAs of the WKYs (Fig. 8c). The normalization of FNDC5 expression by miR-135a-5p knockdown was further confirmed by immunohistochemical analysis (Fig. 8d), and obvious changes in FNDC5 expression (brown color) were observed in the vascular smooth muscle of the arterial media (Fig. 8e).

Effects of miR-135a-5p knockdown on PCNA expression and vascular remodeling

Immunohistochemical analysis of PCNA showed that miR-135a-5p knockdown prevented the upregulation of PCNA in the aortas of the SHRs (Fig. 9a), and obvious changes in the expression of PCNA

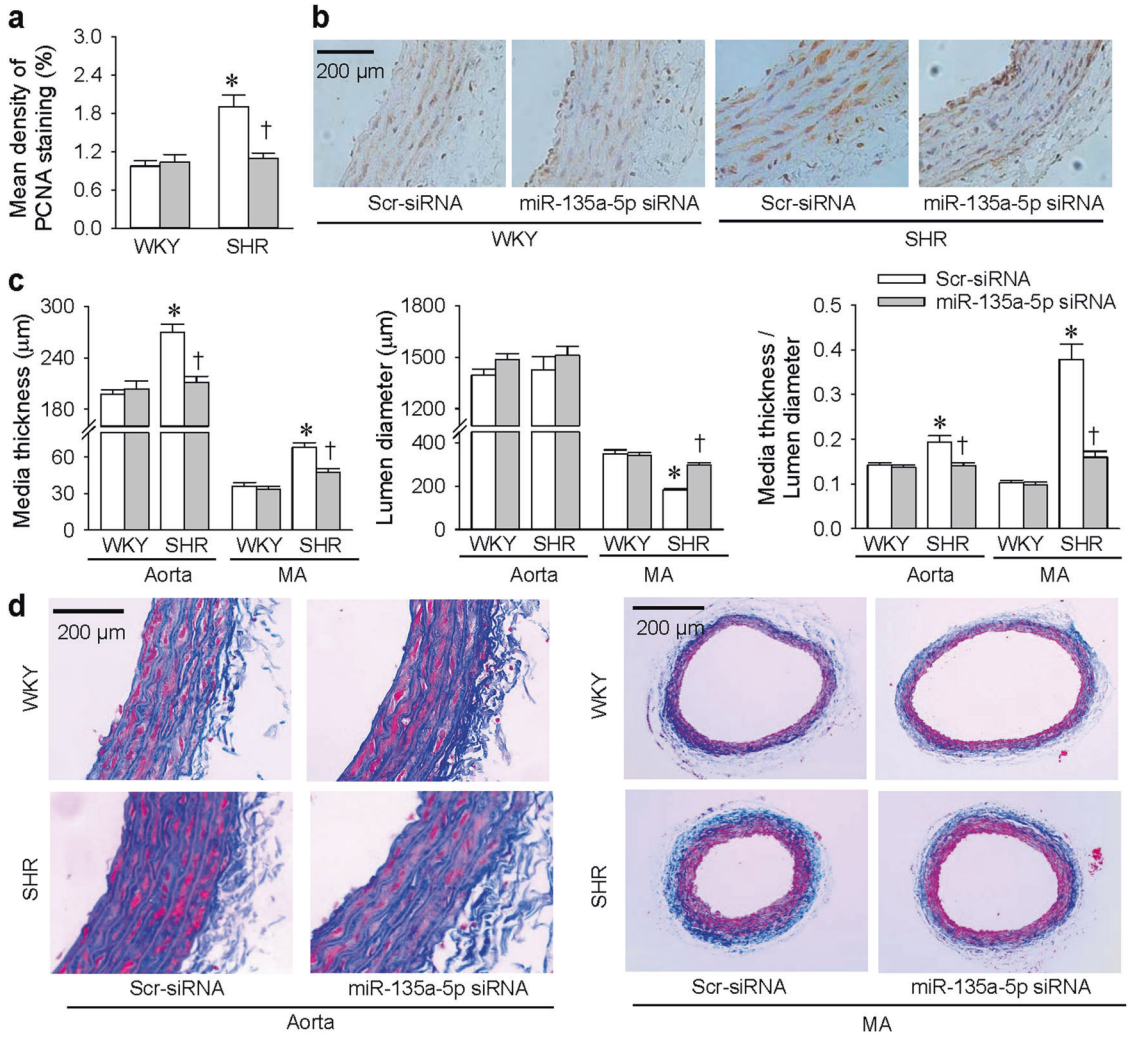

Fig. 9 Effects of miR-135a-5p knockdown in WKYs and SHRs on PCNA expression and vascular remodeling. Measurements were made 3 weeks after the intravenous administration of control lentivirus (Scr-siRNA) or miR-135a-5p siRNA lentivirus (miR-135a-5p siRNA, 2×10^{11} plaque forming units/mL, 100 μL). **a** Bar graph showing the relative densities of PCNA staining in the aortas. **b** Representative images of immunohistochemical analysis of PCNA (brown color) in the aortas. **c** Bar graph showing Masson's staining analysis of media thickness, lumen diameter, and their ratio in the aortas and mesenteric arteries (MAs). **d** Representative images of Masson's staining of the aortas and MAs. The values are the mean ± SEM. $^{*}P < 0.05$ vs WKY. $^{\dagger}P < 0.05$ vs Scr-siRNA. $n = 6$

(brown color) were observed in the vascular smooth muscle of the arterial media (Fig. 9b). Vascular remodeling was evaluated in the aortas and MAs with Masson's staining. The increased media thickness, media thickness/lumen diameter ratio, and media cross-sectional area in the aortas and MAs of the SHRs were attenuated by miR-135a-5p knockdown. The reduced lumen diameter of the MAs was attenuated by miR-135a-5p knockdown (Fig. 9c, d and Supplementary Fig. S6a). Furthermore, the increased outer diameter of the aortas and reduced outer diameter of the MAs were attenuated by miR-135a-5p knockdown (Supplementary Fig. S6b). These results indicate that the inhibition of miR-135a-5p production attenuates vascular smooth muscle proliferation, vascular remodeling, and hypertension in SHRs.

DISCUSSION

VSMC proliferation is important for vascular remodeling during hypertension [3]. We have shown that miR-155-5p inhibits VSMC proliferation by inhibiting ACE expression in SHRs [9]. Here, we found that another miRNA, miR-135a-5p, promotes VSMC proliferation in SHRs. The primary novel findings of this study are that increased miR-135a-5p levels in SHRs exacerbates VSMC proliferation in SHRs by downregulating FNDC5 expression. Silencing miR-135a-5p attenuates VSMC proliferation and vascular remodeling in SHRs by normalizing FNDC5 expression.

Previous studies have shown that miR-135a-5p is involved in the proliferation of cancer cells [11–13]. We found that the miR-135a-5p level was increased in the VSMCs of SHRs. MiR-135a-5p promotes VSMC proliferation, while the inhibition or knockdown of miR-135a-5p inhibits the proliferation of VSMCs in SHRs. Furthermore, miR-135a-5p knockdown in SHRs inhibits vascular remodeling. Both the in vivo and in vitro findings indicate that the increased miR-135a-5p level in the VSMCs of SHRs contributes to the proliferation of VSMCs from SHRs. Intervention of miR-135a-5p may be a therapeutic strategy for attenuating vascular remodeling. Hypertension is associated with vascular remodeling, which has an impact on cardiovascular prognosis, and inhibition of excessive VSMC proliferation is beneficial for attenuating hypertension [33]. We noted that the anti-hypertensive effect of miR-135a-5p knockdown occurred 2 weeks after transfection,

suggesting that the anti-hypertensive effect may be secondary to the attenuation of vascular remodeling. Moreover, the attenuation of hypertension may be beneficial for the improvement of vascular remodeling in SHRs.

FNDC5 is important in metabolic homeostasis and is associated with the pathogenesis of metabolic disorders [34–36]. We found that FNDC5 expression was reduced in the VSMCs of SHRs. Either exogenous FNDC5 or FNDC5 overexpression attenuated VSMC proliferation in SHRs, while FNDC5 knockdown promoted VSMC proliferation in SHRs. The findings suggest that FNDC5 upregulation may be another strategy for inhibiting VSMC proliferation in SHRs. FNDC5 attenuates oxidative stress and inflammation in doxorubicin-treated cardiomyocytes [37]. We have shown that FNDC5 inhibits oxidative stress and inflammation in the AFs of SHRs [20] and attenuates oxidized low-density lipoprotein-induced foam cell formation, monocyte adhesion, and inflammation in VSMCs [38]. More recently, FNDC5 was shown to inhibit oxidative stress and NLRP3 inflammasome activation in VSMCs via the AMPK-SIRT1 signaling pathway [39]. These findings suggest that the roles of FNDC5 in attenuating oxidative stress and inflammation may be partially attributed to the effects of miR-135a-5p on VSMC proliferation.

Interestingly, miR-135a-5p affects VSMC proliferation only in SHRs but not in WKYs. A possible mechanism is that the role of miR-135a-5p-mediated FNDC5 downregulation in promoting VSMC proliferation may be counteracted by some compensatory mechanisms that inhibit VSMC proliferation in order to maintain a normal proliferation state in WKYs. However, the proliferation-promoting effect is greatly enhanced due to increased angiotensin II production and enhanced oxidative stress and inflammation [23, 24] in the VSMCs of SHRs, while FNDC5 is an important factor in counteracting the VSMC proliferation of SHRs. Thus, increased miR-135a-5p levels in SHRs inhibit FNDC5 expression and thereby promote VSMC proliferation, and miR-135a-5p inhibition in SHRs normalizes FNDC5 expression and then attenuates VSMC proliferation.

This study provides solid evidence that miR-135a-5p deteriorates VSMC proliferation in SHRs by inhibiting FNDC5 expression, while silencing miR-135a-5p attenuates VSMC proliferation and vascular remodeling in SHRs via the recovery of FNDC5 expression; these findings indicate the importance of miR-135a-5p in the pathogenesis of hypertension. Our previous study showed that FNDC5/irisin attenuates insulin resistance, glucose and lipid metabolism disorders, and hepatosteatosis [16–18]. Inhibition of miR-135a-5p-induced FNDC5 normalization not only attenuates vascular remodeling and hypertension but also may improve glucose and lipid metabolism and insulin resistance. Therefore, intervention of miR-135a-5p may be a strategy with some unique advantages for attenuating the vascular remodeling and hypertension associated with obesity, diabetes, atherosclerosis, hepatosteatosis, and some other metabolic disorders; this hypothesis requires further investigation.

In summary, the miR-135a-5p level is increased while FNDC5 expression is decreased in the VSMCs from SHRs. MiR-135a-5p promotes the proliferation of VSMCs from SHRs by inhibiting FNDC5 expression. Inhibition of miR-135a-5p attenuates the proliferation of VSMCs from SHRs via the normalization of FNDC5 expression. MiR-135a-5p knockdown normalizes FNDC5 expression and attenuates vascular smooth muscle proliferation, vascular remodeling, and hypertension in SHRs. This study shows the crucial role of increased miR-135a-5p levels in promoting VSMC proliferation in SHRs. Both miR-135a-5p and FNDC5 might be crucial targets for attenuating VSMC proliferation in hypertension.

ACKNOWLEDGEMENTS

This study was supported by the National Natural Science Foundation of China [32071106, 91639105, 31871148, and 81770426].

AUTHOR CONTRIBUTIONS

CY, YT, QC, YHL, YMK, and GQZ designed experiments. CY, YT, NW, GWW, FZ, JZL, HZ, and ADC conducted the experiments. CY, YT, NW, GWW, JYC, JJW, and GQZ performed data and statistical analyses. CY, YT, and GQZ wrote the manuscript, with contributions from all the other authors. GQZ supervised the study. All authors approved the final version for submission.

ADDITIONAL INFORMATION

Supplementary information The online version contains supplementary material available at https://doi.org/10.1038/s41401-020-00608-x.

Competing interests: The authors declare no competing interests.

REFERENCES

1. Rizzoni D, Agabiti RE. Small artery remodeling in hypertension and diabetes. Curr Hypertens Rep. 2006;8:90–5.
2. Wang D, Uhrin P, Mocan A, Waltenberger B, Breuss JM, Tewari D, et al. Vascular smooth muscle cell proliferation as a therapeutic target. Part 1: molecular targets and pathways. Biotechnol Adv. 2018;36:1586–607.
3. Schiffrin EL. Vascular remodeling in hypertension: mechanisms and treatment. Hypertension. 2012;59:367–74.
4. Brown IAM, Diederich L, Good ME, DeLalio LJ, Murphy SA, Cortese-Krott MM, et al. Vascular smooth muscle remodeling in conductive and resistance arteries in hypertension. Arterioscler Thromb Vasc Biol. 2018;38:1969–85.
5. Pu M, Chen J, Tao Z, Miao L, Qi X, Wang Y, et al. Regulatory network of miRNA on its target: coordination between transcriptional and post-transcriptional regulation of gene expression. Cell Mol Life Sci. 2019;76:441–51.
6. Dong Y, Liu C, Zhao Y, Ponnusamy M, Li P, Wang K. Role of noncoding RNAs in regulation of cardiac cell death and cardiovascular diseases. Cell Mol Life Sci. 2018;75:291–300.
7. Zhou SS, Jin JP, Wang JQ, Zhang ZG, Freedman JH, Zheng Y, et al. miRNAS in cardiovascular diseases: potential biomarkers, therapeutic targets and challenges. Acta Pharmacol Sin. 2018;39:1073–84.
8. Song XW, Zou LL, Cui L, Li SH, Qin YW, Zhao XX, et al. Plasma miR-451 with echocardiography serves as a diagnostic reference for pulmonary hypertension. Acta Pharmacol Sin. 2018;39:1208–16.
9. Ren XS, Tong Y, Qiu Y, Ye C, Wu N, Xiong XQ, et al. MiR155-5p in adventitial fibroblasts-derived extracellular vesicles inhibits vascular smooth muscle cell proliferation via suppressing angiotensin-converting enzyme expression. J Extracell Vesicles. 2020;9:1698795.
10. Tong Y, Ye C, Ren XS, Qiu Y, Zang YH, Xiong XQ, et al. Exosome-mediated transfer of ACE (angiotensin-converting enzyme) from adventitial fibroblasts of spontaneously hypertensive rats promotes vascular smooth muscle cell migration. Hypertension. 2018;72:881–8.
11. Zhang Y, Jiang WL, Yang JY, Huang J, Kang G, Hu HB, et al. Downregulation of lysyl oxidase-like 4 LOXL4 by miR-135a-5p promotes lung cancer progression in vitro and in vivo. J Cell Physiol. 2019;234:18679–87.
12. Gao S, Yang D, Huang W, Wang T, Li W. miR-135a-5p affects adipogenic differentiation of human adipose-derived mesenchymal stem cells by promoting the Hippo signaling pathway. Int J Clin Exp Pathol. 2018;11:1347–55.
13. Guo LM, Ding GF, Xu W, Ge H, Jiang Y, Chen XJ, et al. MiR-135a-5p represses proliferation of HNSCC by targeting HOXA10. Cancer Biol Ther. 2018;19:973–83.
14. Zhao X, Sun Z, Li H, Jiang F, Zhou J, Zhang L. MiR-135a-5p modulates biological functions of thyroid carcinoma cells via targeting VCAN 3′-UTR. Cancer Biomark. 2017;20:207–16.
15. Bostrom P, Wu J, Jedrychowski MP, Korde A, Ye L, Lo JC, et al. A PGC1-alpha-dependent myokine that drives brown-fat-like development of white fat and thermogenesis. Nature. 2012;481:463–8.
16. Xiong XQ, Chen D, Sun HJ, Ding L, Wang JJ, Chen Q, et al. FNDC5 overexpression and irisin ameliorates glucose/lipid metabolic derangements and enhances lipolysis in obesity. Biochim Biophys Acta. 2015;1852:1867–75.
17. Liu TY, Shi CX, Gao R, Sun HJ, Xiong XQ, Ding L, et al. Irisin inhibits hepatic gluconeogenesis and increases glycogen synthesis via the PI3K/Akt pathway in type 2 diabetic mice and hepatocytes. Clin Sci (Lond). 2015;129:839–50.
18. Liu TY, Xiong XQ, Ren XS, Zhao MX, Shi CX, Wang JJ, et al. FNDC5 alleviates hepatosteatosis by restoring AMPK/mTOR-mediated autophagy, fatty acid oxidation, and lipogenesis in mice. Diabetes. 2016;65:3262–75.
19. Xiong XQ, Geng Z, Zhou B, Zhang F, Han Y, Zhou YB, et al. FNDC5 attenuates adipose tissue inflammation and insulin resistance via AMPK-mediated macrophage polarization in obesity. Metabolism. 2018;83:31–41.
20. Ling L, Chen D, Tong Y, Zang YH, Ren XS, Zhou H, et al. Fibronectin type III domain containing 5 attenuates inflammasome activation and phenotypic

transformation of adventitial fibroblasts in spontaneously hypertensive rats. J Hypertens. 2018;36:1104–14.
21. Liao Q, Qu S, Tang LX, Li LP, He DF, Zeng CY, et al. Irisin exerts a therapeutic effect against myocardial infarction via promoting angiogenesis. Acta Pharmacol Sin. 2019;40:1314–21.
22. Sun HJ, Zhao MX, Ren XS, Liu TY, Chen Q, Li YH, et al. Salusin-beta promotes vascular smooth muscle cell migration and intimal hyperplasia after vascular injury via ROS/NFkappaB/MMP-9 pathway. Antioxid Redox Signal. 2016;24:1045–57.
23. Sun HJ, Ren XS, Xiong XQ, Chen YZ, Zhao MX, Wang JJ, et al. NLRP3 inflammasome activation contributes to VSMC phenotypic transformation and proliferation in hypertension. Cell Death Dis. 2017;8:e3074.
24. Chen D, Zang YH, Qiu Y, Zhang F, Chen AD, Wang JJ, et al. BCL6 attenuates proliferation and oxidative stress of vascular smooth muscle cells in hypertension. Oxid Med Cell Longev. 2019;2019:5018410.
25. Fan ZD, Zhang L, Shi Z, Gan XB, Gao XY, Zhu GQ. Artificial microRNA interference targeting AT1a receptors in paraventricular nucleus attenuates hypertension in rats. Gene Ther. 2012;19:810–7.
26. Zhang LL, Ding L, Zhang F, Gao R, Chen Q, Li YH, et al. Salusin-beta in rostral ventrolateral medulla increases sympathetic outflow and blood pressure via superoxide anions in hypertensive rats. J Hypertens. 2014;32:1059–67.
27. Zhang Y, Qian X, Sun X, Lin C, Jing Y, Yao Y, et al. Liuwei Dihuang, a traditional Chinese medicinal formula, inhibits proliferation and migration of vascular smooth muscle cells via modulation of estrogen receptors. Int J Mol Med. 2018;42:31–40.
28. Hedin U, Thyberg J. Plasma fibronectin promotes modulation of arterial smooth-muscle cells from contractile to synthetic phenotype. Differentiation. 1987;33:239–46.
29. Sotomayor-Flores C, Rivera-Mejias P, Vasquez-Trincado C, Lopez-Crisosto C, Morales PE, Pennanen C, et al. Angiotensin-(1-9) prevents cardiomyocyte hypertrophy by controlling mitochondrial dynamics via miR-129-3p/PKIA pathway. Cell Death Differ. 2020;27:2586–604.
30. Pennanen C, Parra V, Lopez-Crisosto C, Morales PE, Del CA, Gutierrez T, et al. Mitochondrial fission is required for cardiomyocyte hypertrophy mediated by a Ca^{2+}-calcineurin signaling pathway. J Cell Sci. 2014;127:2659–71.
31. Zhang KL, Shen QQ, Fang YF, Sun YM, Ding J, Chen Y. AZD9291 inactivates the PRC2 complex to mediate tumor growth inhibition. Acta Pharmacol Sin. 2019;40:1587–95.
32. Wang D, Ren J, Ren H, Fu JL, Yu D. MicroRNA-132 suppresses cell proliferation in human breast cancer by directly targeting FOXA1. Acta Pharmacol Sin. 2018;39:124–31.
33. Briet M, Schiffrin EL. Treatment of arterial remodeling in essential hypertension. Curr Hypertens Rep. 2013;15:3–9.
34. Cao RY, Zheng H, Redfearn D, Yang J. FNDC5: a novel player in metabolism and metabolic syndrome. Biochimie. 2019;158:111–6.
35. Polyzos SA, Anastasilakis AD, Efstathiadou ZA, Makras P, Perakakis N, Kountouras J, et al. Irisin in metabolic diseases. Endocrine. 2018;59:260–74.
36. Panati K, Suneetha Y, Narala VR. Irisin/FNDC5—an updated review. Eur Rev Med Pharmacol Sci. 2016;20:689–97.
37. Zhang X, Hu C, Kong CY, Song P, Wu HM, Xu SC, et al. FNDC5 alleviates oxidative stress and cardiomyocyte apoptosis in doxorubicin-induced cardiotoxicity via activating AKT. Cell Death Differ. 2020;27:540–55.
38. Zang YH, Chen D, Zhou B, Chen AD, Wang JJ, Gao XY, et al. FNDC5 inhibits foam cell formation and monocyte adhesion in vascular smooth muscle cells via suppressing NFκB-mediated NLRP3 upregulation. Vasc Pharmacol. 2019;121:106579.
39. Zhou B, Qiu Y, Wu N, Chen AD, Zhou H, Chen Q, et al. FNDC5 attenuates oxidative stress and NLRP3 inflammasome activation in vascular smooth muscle cells via activating the AMPK-SIRT1 signal pathway. Oxid Med Cell Longev. 2020;2020:6384803.